High-precision Visual Servoing in Asteroid Flyby with Multirate Feedforward Control and Trajectory Estimation

Yusuke Ogata, Hiroshi Fujimoto, and Yoichi Hori
The University of Tokyo
5-1-5, Kashiwanoha, Kashiwa, Chiba, 277-8561, Japan
Phone: +81-4-7136-3881
Email: ogata.yusuke20@ae.k.u-tokyo.ac.jp, fujimoto@k.u-tokyo.ac.jp, hori@k.u-tokyo.ac.jp

2021 IEEE International Conference on Mechatronics (ICM) | 978-1-7281-4442-9/21/$31.00 ©2021 IEEE | DOI: 10.1109/ICM46511.2021.9385625

***Abstract*—In the flyby search for an asteroid, it is necessary to precisely direct the observation mirror to the viewing angle, which changes significantly at the closest approach point. In order to develop a control law for the mirror, we have to deal with the quantization due to resolution of the camera and dead time due to image processing. This paper proposes an application of multirate feedforward control based on the estimation of relative trajectory. The proposed method reduces the tracking error generated by the influence of quantization noise and enables to keep the angular error within one pixel or less by using an estimation of the relative trajectory.**

***Index Terms*—Visual Servo, Multirate Control, Asteroid Flyby, Trajectory Estimation**

I. Introduction

A. Necessity of Asteroid Exploration and Flyby Observations

Exploration of the solar system by space probes is one of the most effective ways to search for the origin of the solar system, and many space probes have been launched by various countries since the launch of the Soviet Union's Luna 1 in 1959. Many space probes have been launched also in Japan to explore the solar system, from Sakigake, which was launched in 1985 to Hayabusa2, which is currently in operation [1]. There are several methods of solar system exploration, and flyby observation is one of them. Flyby observations are performed using onboard cameras when a spacecraft passes through the vicinity of a target planet or asteroid. The amount of obtained information is small compared with methods such as sample return, which brings back samples directly from the target. However, many asteroids cannot be observed by other methods than flyby due to constraints of their trajectories such as large eccentricity, so that flyby is the still important exploration method [2].

B. Asteroid Explorer DESTINY+

DESTINY+ is a deep space probe being developed by Japan Aerospace Exploration Agency (JAXA) for launch in 2024 [2], which is the main application of this study. Telescopic CAmera for Phaeton (TCAP) onboard the space probe will be used to take images of the asteroid named 3200 Phaeton. One engineering mission of DESTINY+ is to acquire advanced techniques for flyby exploration through this flyby observation.

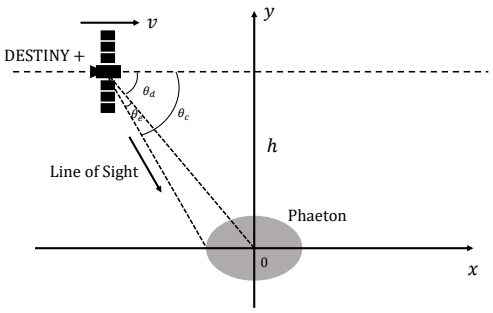

Fig. 1. Schematic diagram of flyby by DESTINY+

In this paper, each parameter is set assuming that TCAP will take pictures of 3200 Phaeton.

C. Issues and Proposed Method

During flyby observations, cameras or mirrors that relay images must point at a target accurately, and it is important to suppress the angular error that causes the positional error and the angular velocity error that leads to blur. Recently, high-resolution cameras and various conditions of trajectory made it difficult to meet the strict requirements of pointing accuracy. Therefore, research and development of high-precision ($\approx 1 \times 10^{-4}$ deg) pointing control algorithms are required in DESTINY+. It is difficult to obtain the detailed relative trajectory of the asteroid and the spacecraft in advance, so estimating it is indispensable to accurate tracking.

In the past, PD control has been mainly used based on calculating the angular error from captured images without estimating the relative trajectory [3]. The feedback period is limited by the imaging period of the camera which is the slowest in the system. Furthermore, no compensation is made for dead time in image processing, which deteriorates the tracking performance near the closest point of the asteroid where the target angular velocity changes significantly.

In the previous study of relative trajectory estimation [4], the velocity parameters (v_x, v_y, v_z) were estimated in the three-dimensional Cartesian coordinate system in order to avoid the deterioration of tracking performance led to by dead

978-1-7281-4442-9/21/$31.00 ©2021 IEEE

TABLE I
NOMINAL ORBIT PARAMETERS OF DESTINY+

Discription	Symbol	Value
Relative speed	v	33 km/s
Closest approach distance	h	500 km
Closest approach time	t_0	0 s

time in the image-based feedback. However, the estimation of three variables is redundant because the target angle is uniquely determined by two variables, the distance between the spacecraft's current position and the closest approach point of the asteroid, and the closest approach distance. Besides, the noise caused by the quantization of images is not discussed. Relative position estimation between the spacecraft and the asteroid by particle filter [5] uses the diameter of target asteroid and the relative velocity, which have uncertainties.

Our research group have been studying visual servoing using a robotic arm [6], and high-precision positioning control for discrete-time systems such as semiconductor manufacturing apparatus [7]. The problems in visual servo systems, in which the image capturing period is long and the image processing generates dead time, have been solved by applying multirate control and dead time compensation [8], [9]. We have also shown that it is possible to follow a target trajectory with high accuracy even in the presence of unknown parameters in a plant [10].

This paper proposes a new control method in flyby to improve the control performance significantly over the conventional method. This method combines multirate feedforward control and the trajectory estimation algorithm using Recursive Least Squares (RLS). It reduces the blur caused by angular error and angular velocity error during imaging to within one pixel.

The structure of this paper is as follows. In Section II, we derive the target trajectory by modeling the relative motion between DESTINY+ and Phaeton and required accuracy by TCAP parameters. The estimation and control law is proposed in Section III. We simulate the proposed method in Section IV and experimental result is presented in Section V. Conclusion is given in Section VI.

II. Modeling Asteroid Flyby Conditions with DESTINY+

During the flyby, DESTINY+ is considered to have a linear uniform motion with respect to Phaeton like Fig. 1. Trajectory parameters assumed in this case are shown in Table I.

Under these conditions, the angle θ_d and the angular velocity ω_d to which the camera should be directed are given by Eq. (1) – Eq. (3).

$$\theta_d(t) = \begin{cases} -\arctan\left(\frac{h_v}{t}\right) & \text{if} \quad t < 0 \\ \pi - \arctan\left(\frac{h_v}{t}\right) & \text{else} \end{cases} \tag{1}$$

$$\omega_d(t) = \frac{h_v}{t^2 + (h_v)^2} \tag{2}$$

$$h_v := h/v \tag{3}$$

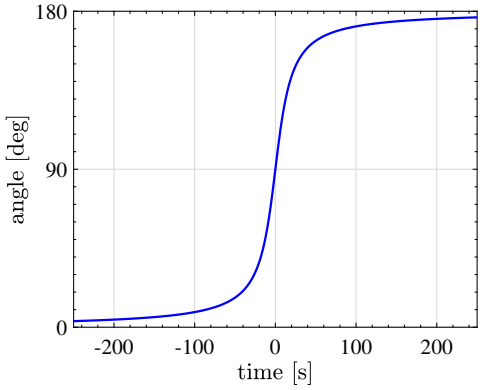

Fig. 2. Trajectory of angle

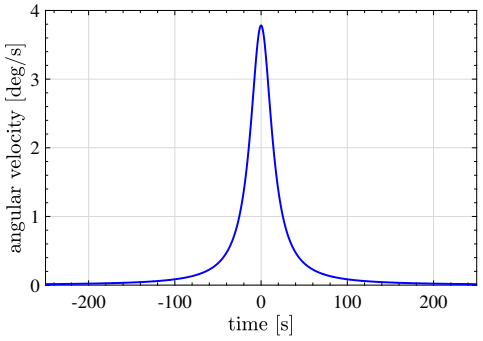

Fig. 3. Trajectory of angular velocity

The trajectory of θ_d and ω_d are shown in Fig. 2 – Fig. 3.

As shown in Fig. 2, the angle of TCAP changes drastically 250 s before and after the closest approaching time. Conventional PD control [3] cannot keep up with the angle change and causes a large angular error.

Also, TCAP parameters used in the DESTINY+ are shown in Table II [3].

Based on the angular resolution and exposure time in Table II, if the angular error at the beginning of exposure is reduced to less than 3.3×10^{-4} deg and the angular velocity error is reduced to less than 1.1 deg/s, the center of the image coincides with the center of Phaeton and there is no blur during exposure time, then ideal images can be obtained.

Approximating the speed inner-loop as a first-order delay with time constant τ, the transfer function $P(s)$ from the reference velocity ω^* to the output angle θ of the driving mirror is modeled as follows:

$$P(s) = \frac{1}{s(\tau s + 1)}. \tag{4}$$

Friction and other disturbances of the motor are compensated by the inner-loop of speed control shown in Fig. 4.

III. Proposed Method of Tracking Asteroid

The proposed control method is shown in Fig. 5. This method consists of two parts: trajectory estimion and reference gereration part, and input gereration part which follows the target value generated in the reference gereration part.

TABLE II
PARAMETERS OF TCAP

Discription	Symbol	Value
Exposure time	T_s	0.3 ms
Camera interval	T_y	0.5 s
Inertia moment	J	0.1 kg · m^2
Angular resolution	Θ_{cam}	3.3×10^{-4} deg/pix
Field of view	Ω	1.1 deg × 0.82 deg

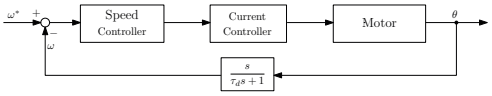

Fig. 4. Inner-loop of the plant $P(s)$

A. Trajectory Estimion and Reference Gereration

1) Estimation of trajectory θ_d: From the relationship between the target trajectory and the camera angle in Fig. 1, the following relationship holds with respect to the tracking error:

$$\theta_e(t) = \theta_c(t) - \theta_d(t), \tag{5}$$

where θ_c is the angle of the mirror to the direction of the spacecraft's velocity and θ_e is tracking error of TCAP obtained from images. θ_c can be taken from the encoder of TCAP, and θ_e can be taken from image processing. By deforming this and considering dead time T_d for image processing to get the center of Phaeton, we obtain the following equation as the past target trajectory which is T_d before current time t:

$$\hat{\theta}_d(iT_y - T_d) = \theta_c(iT_y - T_d) - \theta_e[i], \tag{6}$$

where i is an output index, T_y is an imaging period and $\theta_e[i] = \theta_e(iT_y)$. The sampling period of the encoder is short enough compared to the camera that $\theta_c(iT_y - T_d)$ can be obtained for any T_d. So correct estimation is possible even in the presence of dead time caused by image processing.

2) Estimation of Trajectory Parameter: Based on the obtained $\hat{\theta}_d(t)$, parameters that determine the trajectory are estimated. From Eq. (1), the function to be fitted is determined as follows:

$$\hat{\theta}_d(t) = \begin{cases} -\arctan\left(\frac{h_v}{t-t_0}\right) & \text{if} \quad t < t_0 \\ \pi - \arctan\left(\frac{h_v}{t-t_0}\right) & \text{else.} \end{cases} \tag{7}$$

The two parameters, h_v and t_0, are estimated. Each parameter determine the shape of trajectory and the time of closest approach. By taking tangent on both sides of Eq. (7), the following linear relationship for the estimation parameter is obtained:

$$(\tan\hat{\theta}_d)t = \begin{bmatrix} -1 & \tan\hat{\theta}_d \end{bmatrix} \begin{bmatrix} \theta_1 \\ \theta_2 \end{bmatrix} \tag{8}$$

$$\theta_1 = h_v \tag{9}$$

$$\theta_2 = t_0. \tag{10}$$

RLS is applied to the estimation, and an update formula is expressed by Eq. (11) – Eq. (12). Here, $\boldsymbol{\phi}[i]$ is a regressor, $\boldsymbol{\theta}[i] = [\theta_1 \ \theta_2]^t$ is an estimation parameter vector, $\boldsymbol{P}[i]$ is an error covariance matrix, and y is an output.

$$\boldsymbol{\theta}[i] = \boldsymbol{\theta}[i-1] + \frac{\boldsymbol{P}[i-1]\boldsymbol{\phi}[i]}{\lambda + \boldsymbol{\phi}^t[i]\boldsymbol{P}[i-1]\boldsymbol{\phi}[i]}(y - \boldsymbol{\phi}[i]\boldsymbol{\theta}[i-1]) \tag{11}$$

$$\boldsymbol{P}[i] = \frac{1}{\lambda}\left(\boldsymbol{P}[i-1] - \frac{\boldsymbol{P}[i-1]\boldsymbol{\phi}[i]\boldsymbol{\phi}^t[i]\boldsymbol{P}[i-1]}{1 + \boldsymbol{\phi}[i]\boldsymbol{P}[i-1]\boldsymbol{\phi}[i]}\right) \tag{12}$$

FromEq. (8) and Eq. (11), the trajectory parameter $\boldsymbol{\theta}[i]$ can be estimated for each index i.

3) Reference Generation: From the obtained θ_1, θ_2 and the current time t, the angle reference $\theta_{ref}[i+1]$ and the angular velocity reference $\omega_{ref}[i+1]$ at the next reference sampling time $t = (i+1)T_r$ are calculated as follows:

$$\theta_{ref}[i+1] = \begin{cases} -\arctan\left(\frac{\hat{h}_v}{t-\hat{t}_0+T_r}\right) & \text{if} \quad t + T_r < \hat{t}_0 \\ \pi - \arctan\left(\frac{\hat{h}_v}{t-\hat{t}_0+T_r}\right) & \text{else} \end{cases} \tag{13}$$

$$\omega_{ref}[i+1] = \frac{\hat{h}_v}{(t - \hat{t}_0 + T_r)^2 + (\hat{h}_v)^2}. \tag{14}$$

B. Input Generation

Applying the multirate feedforward control [11] , the angle and the angular velocity of the mirror are perfectly tracked to the reference generated by the reference generator in each sampling period of the camera. State equation of the plant Eq. (4) in continuous time is expressed as follows:

$$\begin{aligned} \dot{\boldsymbol{x}}(t) &= \boldsymbol{A}_c\boldsymbol{x}(t) + \boldsymbol{b}_c u(t) \\ y(t) &= \boldsymbol{c}_c\boldsymbol{x}(t). \end{aligned} \tag{15}$$

Eq. (15) can be discretized as shown below by multirate sampling with two input switching per a reference sampling period T_r:

$$\begin{aligned} \boldsymbol{x}[i+1] &= \boldsymbol{A}\boldsymbol{x}[i] + \boldsymbol{B}\boldsymbol{u}[i] \\ \boldsymbol{y}[i] &= \boldsymbol{C}\boldsymbol{x}[i] + \boldsymbol{D}\boldsymbol{u}[i] \end{aligned} \tag{16}$$

$$\boldsymbol{A} = e^{\boldsymbol{A}_c T_r} \tag{17}$$

$$\boldsymbol{B} = \begin{bmatrix} \int_{\frac{1}{2}T_r}^{T_r} e^{\boldsymbol{A}_c\tau}\boldsymbol{b}_c d\tau & \int_0^{\frac{1}{2}T_r} e^{\boldsymbol{A}_c\tau}\boldsymbol{b}_c d\tau \end{bmatrix} \tag{18}$$

$$\boldsymbol{C} = \begin{bmatrix} \boldsymbol{c}_c & \boldsymbol{c}_c e^{\boldsymbol{A}_c \frac{1}{2}T_r} \end{bmatrix} \tag{19}$$

$$\boldsymbol{D} = \begin{bmatrix} 0 & 0 \\ \int_0^{\frac{1}{2}T_r} e^{\boldsymbol{A}_c\tau}\boldsymbol{b}_c d\tau & 0 \end{bmatrix}. \tag{20}$$

The following feedforward controller is configured for the discretized plant Eq. (16):

$$C_1[z] = \boldsymbol{B}^{-1}\left(\boldsymbol{I} - z^{-1}\boldsymbol{A}\right), \tag{21}$$

where $z = e^{sT_r}$. By inputting $\boldsymbol{x}_{ref}[i+1]$ into the feedforward controller $C_1[z]$, the state is fully tracked to the reference value as $\boldsymbol{x}[i+1] = \boldsymbol{x}_{ref}[i+1]$ if there is no modeling error of the plant. The angular error between the output and the reference generated by the modeling error is compensated by the feedback controller $C_2[z]$ in Fig. 5, and PID controller is used as $C_2[z]$ in this paper.

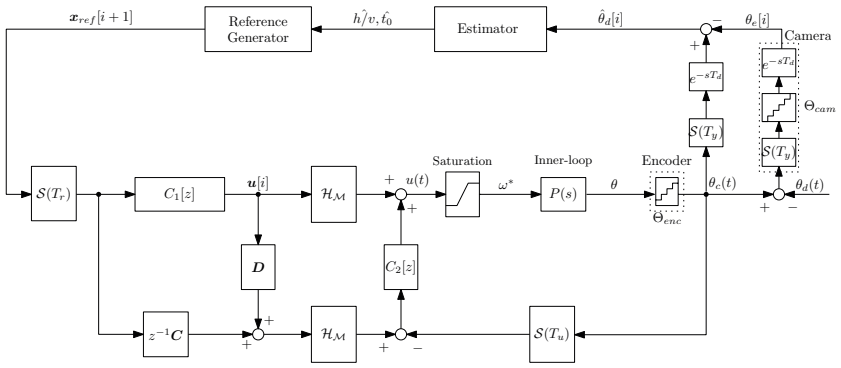

Fig. 5. Block diagram of proposed method

TABLE III
SIMULATION CONDITIONS OF THE PROPOSED METHOD

Description	Symbol	Value
Time constant of the inner-loop	τ	0.05 s
Resolution of encoder	Θ_{enc}	3.32×10^{-5} deg
Input period	T_u	1.0×10^{-3} s
Reference sampling period	T_r	2.0×10^{-3} s
Imaging period	T_y	0.5 s
Dead time	T_d	0.1 s
Initial value of $\hat{h}_v$		15.1545 s
Initial value of $\hat{t}_0$		1.0×10^{-3} s
Forgetting factor	λ	0.99
Initial value of $\boldsymbol{P}[i]$	$\boldsymbol{P}[0]$	diag(0.1, 0.1)

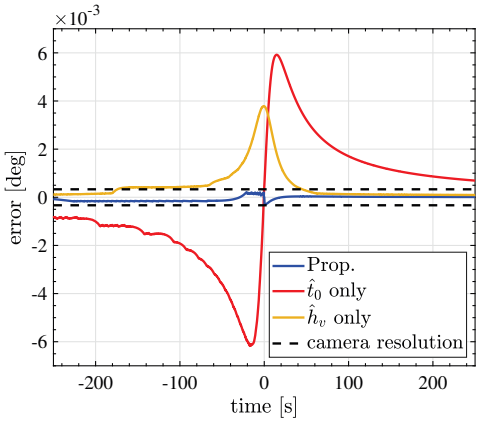

Fig. 6. Angular error (Simulation)

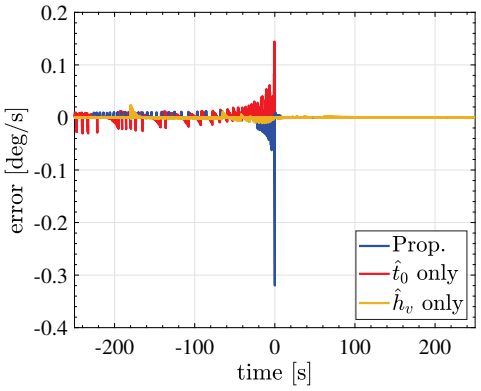

Fig. 7. Angular velocity error (Simulation)

IV. SIMULATION OF PROPOSED METHOD

A. Simulation Condition

Simulations were performed by MATLAB/Simulink® to confirm the control performance achieved by the proposed method. Simulation conditions were set as shown in Table I – Table III. As it can be seen from Fig. 3, the angular acceleration increases monotonically toward the nearest approach point, so the forgetting factor was set to $\lambda = 0.99$ to give weight to current information. Initial values of estimating parameters $\hat{t}_0$ and $\hat{h}_v$ were set differently from true values to confirm accuarte estimetion. In this simulation, the modeling error of the plant was ignored and calculations were made from 3500 s before the closest point.

B. Simulation Results

The tracking errors of angle and angular velocity obtained by the simulation are shown in Fig. 6 – Fig. 7. The changes of $\hat{t}_0$ and $\hat{h}_v$ are shown in Fig. 8 – Fig. 9. As a comparison of the control performance, the results when $\hat{t}_0$ is estimated and $\hat{h}_v$ is fixed to 15.1545 s ($\hat{t}_0$ only), and when $\hat{h}_v$ is estimated and $\hat{t}_0$ is fixed to 1.0×10^{-3} s ($\hat{h}_v$ only) are also shown besides the proposed method (Prop.). From Fig. 6, it is shown that the performances of each case when only 1 parameter is estimated are greatly deteriorated by using wrong parameters, even if the errors of the parameters are tiny. On the other hand, the control performance of the proposed method can estimate each parameter accurately as it is shown in Fig. 8 – Fig. 9, and proposed method can achieve high accuracy tracking with less than 1 pixel error. The angular velocity error of the proposed method shown in Fig. 7 has a peak in $t = 0$ because of switching θ_{ref} in Eq. (13). However, the requirement of the angular velocity error of DESTINY+ (1.1 deg/s) is satisfied, and it converges quickly to 0 in $t > 0$.

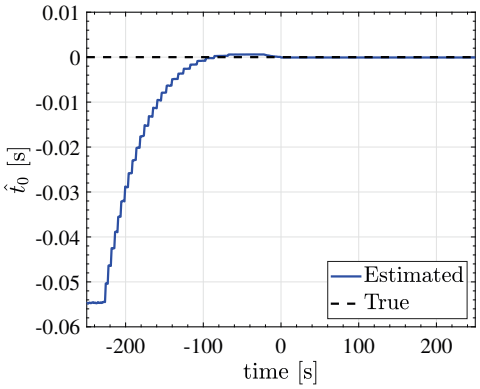

Fig. 8. Estimation parameter $\hat{t}_0$ (Simulation)

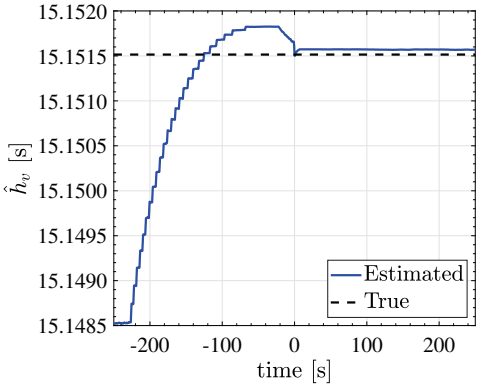

Fig. 9. Estimation parameter $\hat{h}_v$ (Simulation)

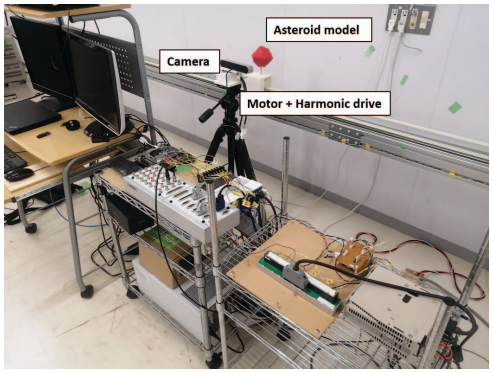

Fig. 10. Experimental setup

TABLE IV
PARAMETERS OF EXPERIMENT DEVICES

Description	Symbol	Value
Resolution of encoder	Θ_{enc}	6.0×10^{-3} deg
Resolution of camera	Θ_{cam}	4.1×10^{-2} deg
Input period	T_u	1.0×10^{-3} s
Reference sampling period	T_r	2.0×10^{-3} s
Imaging period	T_y	0.5 s
Dead time	T_d	0.1 s
Closest distance	h	52.7 cm
Speed of the asteroid	v	3.48 cm/s
Initial value of $\hat{h}_v$		15.15 s
Initial value of $\hat{t}_0$		92 s
Forgetting factor	λ	0.9
Initial value of $\boldsymbol{P}[i]$	$\boldsymbol{P}[0]$	diag(0.1, 0.1)

V. EXPERIMENTS

A. Experimental Setup

To demonstrate effectiveness of the proposed method, experimental setup shown in Fig. 10 was used. Relative motion between a space probe and an asteroid was simulated by fixed camera and moving asteroid. The experiment devices consist of the camera, the motor with Harmonic Drive®, and the asteroid model on the belt drive. Parameters of each component and settings are shown in Table IV. Only left lens of the stereo camera ZED was used as the camera, and the relaying mirror was omitted unlike TCAP. The camera was attached to a position offset to the motor shaft in order that the motor shaft corresponded to the center of the lens. In order to get the center of the asteroid, the center of luminance was calculated after binarization of images. The forgetting factor was set to 0.9 because this experimental setup can only perform estimation for a shorter time than the actual probes.

As a result of system identification, the nominal plant model $P(s)$ is written as follows:

$$P(s) = \frac{191}{s(s+195)}. \tag{22}$$

B. Results

Fig. 11 – Fig. 12 shows the tracking errors of angle and angular velocity. The changes of $\hat{t}_0$ and $\hat{h}_v$ are shown in Fig. 13 – Fig. 14. As in the simulation results, estimation of only one parameter resulted in the large angular error. On the other hand, the angular error could be minimized by estimating two parameters simultaneously in the proposed method. Except for the first few seconds after the start of the experiment, when the camera moved significantly from $\theta_c = 0$ to $\arctan(\hat{h}_v/\hat{t}_0)$, the proposed method was able to keep the angular error within 0.5 deg (12 pix). $\hat{h}_v$ steadily decreased after the closest approach from Fig. 14, but this is not considered to be a problem because from Eq. (13), the estimation error has almost no effect on the angular error in the region where $\theta_c \approx 0$ or π. In this experiment, the estimation was done only for about 90 seconds before the closest approach, so the tracking performance would be better in the actual probes.

VI. CONCLUSION

In this paper, we proposed the high-precision control law for the flyby spacecraft DESTINY+, which is under planning, to keep the angular error within one pixel, even in the closest point, which would cause the large angular error with the conventional PD control.

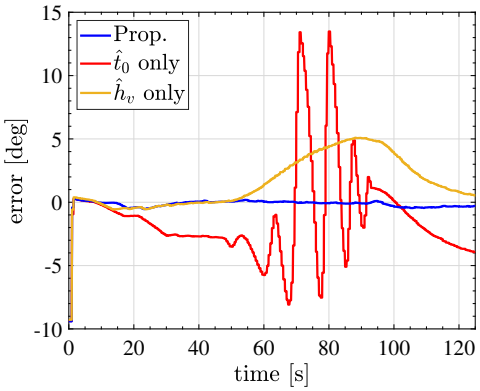

Fig. 11. Angular error (Experiment)

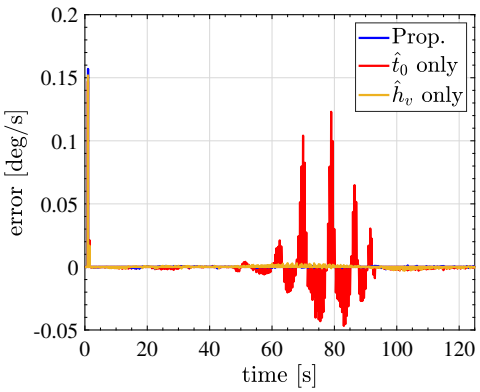

Fig. 12. Angular velocity error (Experiment)

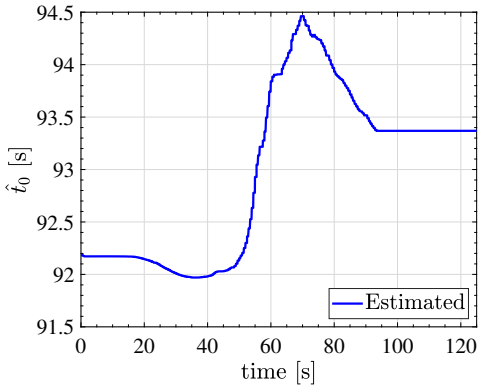

Fig. 13. Estimation parameter $\hat{t}_0$ (Experiment)

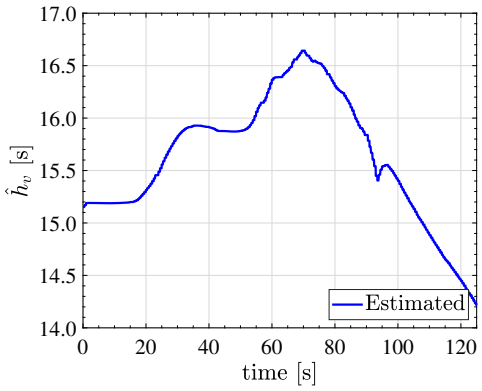

Fig. 14. Estimation parameter $\hat{h}_v$ (Experiment)

We have solved the problem of spatial quantization which is caused by the camera resolution by using images and encoder information to estimate the trajectory. The control performance was evaluated by simulations and experiments, and it was shown that high-precision tracking of target asteroid was achieved by estimation of trajectory parameters in flyby.

As a future work, we need to show the effectiveness of our proposed method in experiments with higher-resolution cameras that more closely resembles the actual device. Since the angular transmission error of the strain wave gearing is on the order of tens of arc seconds [12], the effect of the angular transmission error must be taken into account when using high-resolution cameras. So it is necessary to develop a method to suppress the angular transmission error by using image-based feedback.

References

[1] P. Seguela, *Space Probes: 50 Years of Exploration from Luna 1 to New Horizons*. Firefly Books, 2011.

[2] Japan Aerospace Exploration Agency, "Abstract of destiny+ mission," 2020, https://destiny.isas.jaxa.jp/mission/.

[3] S. Sato, K. Ichinomiya, K. Takemura, T. Chikazawa, K. Ishibashi, and Y. Kawakatsu, "High-speed flyby observation of small asteroid by destiny+," in *[The 28th Workshop on JAXA Astrodynamics and Flight Mechanics 2018]*. Institute of Space and Astronautical Science, Japan Aerospace Exploration Agency(JAXA)(ISAS), 2018.

[4] K. Ariu, T. Inamori, and R. Funase, "Design and demonstration of the visual feedback tracking system for the close asteroid flyby," in *2016 IEEE Aerospace Conference*, 2016, pp. 1–10.

[5] K. Hashizume, K. Miyata, and S. Hara, "Trial report of localization for visual based tracking system in asteroid flyby," *IEEJ Journal of Industry Applications*, vol. advpub, 2020, doi:10.1541/ieejjia.L20000647.

[6] K. Sasajima and H. Fujimoto, "6 dof multirate visual servoing for quick moving objects," in *2007 American Control Conference*, 2007, pp. 1538–1543.

[7] M. Mae, W. Ohnishi, H. Fujimoto, and Y. Hori, "Perfect tracking control considering generalized controllability indices and application for high-precision stage in translation and pitching," *IEEJ Journal of Industry Applications*, vol. 8, no. 2, pp. 263–270, 2019.

[8] H. Fujimoto and Y. Hori, "Visual servoing based on intersample disturbance rejection by multirate sampling control-time delay compensation and experimental verification," in *Proceedings of the 40th IEEE Conference on Decision and Control (Cat. No.01CH37228)*, vol. 1, 2001, pp. 334–339 vol.1.

[9] A. Goto and H. Fujimoto, "Proposal of 6 dof visual servoing of moving object based on real-time distance identification," in *2008 SICE Annual Conference*, 2008, pp. 3208–3213.

[10] H. Fujimoto and Bin Yao, "Multirate adaptive robust control for discrete-time non-minimum phase systems and application to linear motors," *IEEE/ASME Transactions on Mechatronics*, vol. 10, no. 4, pp. 371–377, 2005.

[11] H. Fujimoto, Y. Hori, and A. Kawamura, "Perfect tracking control method based on multirate feedforward control," *Transactions of the Society of Instrument and Control Engineers*, vol. 36, no. 9, pp. 766–772, 2000.

[12] T. V. Trung and M. Iwasaki, "High-performance positioning using decoupling controllers for flexible two-link robots with strain wave gears," *IEEJ Journal of Industry Applications*, vol. 9, no. 4, pp. 408–417, 2020.